

Original Research Article

Research on metal goaf detection: a case study on the Duan Village-Leigou monohydrallite goaf

Zhao Shuxia^{1*}, Wang Wanliang²

¹Chinalco Mining Co. Ltd., Zhengzhou, China

²Chongqing Bureau of Geology and Minerals Exploration, 607 Geological Team, Chongqing, China

Abstract: The increasing scope and depth of mining formed more and more goaves. Geological disasters such as the collapse of goaves demonstrate its hidden danger to people. Therefore, it is particularly important to accurately locate goaves in mining areas. This article studies a section of the Duan Village-Leigou monohydrallite goaf in Mianchi county of Henan Province as an example; using five kinds of detection test including seismic reflection method, direct current method, high density resistivity method, electromagnetic imaging, and radon emanation measurement method. Results from detection and comprehensive analysis of the eight known mine showed that the area is suitable to adopt a high density method when the embedded depth is about 20.0 m or less than 20.0 m, polar distance of which should be 2.0 m. A tunnel buried deep above 20.0 m in the magnetotelluric imaging (EH-4) method is appropriate, choosing a suitable polar distance and dot pitch of 2.0. Through the detection of the Duan Village-Leigou monohydrallite goaf, our research suggests the high density resistivity method and the method of the earth electromagnetic imaging are the most suitable methods to detect the goaf.

Keywords: high density resistivity method; method of earth electromagnetic imaging; radon emanation measurement method; goaf

Citation: Zhao SX, Wang WL. Research on metal goaf detection: A case study on the Duan Village-Leigou monohydrallite goaf. Int J Geol 2016; (1)1: 25–34; <http://dx.doi.org/10.26789/IJG.2016.003>.

*Correspondence to: Zhao Shuxia, Chinalco Mining Co. Ltd., Zhengzhou, China, kyfw@qq.com

Received: 10th June 2016; **Accepted:** 11th July 2016; **Published Online:** 1st September 2016

Introduction

Goaf refers to an empty area left after the underground mineral was excavated, leading to the phenomenon of structure instability^[1]. The physical essence of goaf structural instability is a process of rock medium rupture and instability evolution, destroying the integrity of the overlying rock, which would collapse causing cave-ins, the overlying strata stability destroyed, and the medium in the exploration area locally unstable. Its strength and stiffness is gradually reduced, which will form macroscopic damage under external force at the same time; which in essence is a complex process of physics and mechanics. Goaves can be divided into metal and non-metal goaves according to the character of the mineral resources. The existence of geological disasters in metal goaves such as collapse, subsidence, and so on brought great harm to the mining industry and the lives of residents. At the same time, the hidden dangers in non-metal goaves cannot be ignored. The surface subsidence area caused by China's metal goaves is more than 1150 km²^[1]. Historical volumes of the goaves are more than 250 × 10⁷ m³ and increasing at 10 × 10⁷ m³ every year, causing numerous geological disasters. Hence, it is particularly important to accurately locate metal goaves. This study found detecting goaf

Copyright © 2016 Zhao SX, *et al.* This is an Open Access article distributed under the terms of the Creative Commons Attribution-Non Commercial 4.0 International License (<http://creativecommons.org/licenses/by-nc/4.0/>), permitting all non-commercial use, distribution, and reproduction in any medium, provided the original work is properly cited.

distribution with comprehensive geophysical prospecting methods and comprehensive interpretation on the basis of geological data, by means of drilling verification, could determine the location and spatial distribution of goaves. This would lay a good foundation for the next step and provide a strong basis for evaluation and treatment of goaves^[2,3].

Introduction of existing detection technique

At present, geophysical prospecting method has become the most important technical means of goaf detection^[4,5]. Its main methods are: high density resistivity method, magnetic exploration^[6], electromagnetic prospecting method^[7], multi-channel transient Rayleigh wave^[8,9], goaf detection system, *etc.* Due to complex underground geological environments, the diversity of physical change, the uncertainty of geophysical solution, and other factors, the detection effect of single geophysical method is not ideal. Therefore, it is necessary to synthesize different geophysical methods and make full use of various supporting information. Data from the geophysical field and geological extrapolation should be made to conform to the objective conditions combined with geological and drilling data and other materials.

A lot of domestic work has been done to ascertain underground goaves using geophysical exploration technique in recent years. Goaf detection has become an increasingly difficult problem in engineering geophysics, with many geophysicists researching a variety of methods and techniques. Geophysical methods, according to different geophysical field studies, are usually divided into the following categories (*Figure 1*).

- 1) Based on the density difference of the underground medium, the method of studying gravity field change is called gravity exploration^[10].
- 2) Based on the medium's magnetic difference, the method of studying the change rule of the geomagnetic field is called magnetic exploration^[11].
- 3) Based on the medium's electrical difference, the method of studying the change rule of natural or artificial electric field (or electromagnetic field) is called electrical exploration (or electromagnetic exploration)^[12].
- 4) Based on the medium's elastic difference, the method of studying the change rule of the wave field is called seismic exploration^[13].
- 5) Based on the medium radioactive differences, the method of studying the change characteristics of radiation field is called radioactive exploration^[14].
- 6) Based on the distribution of underground thermal energy and the medium's electrical conductivity, the method of studying the change of the geothermal field is called geothermal measurements^[15].

Detection of Duan Village-Leigou monohydrallite goaf

Overview of the study area

The study area is located in Mianchi County, Henan Province, at the junction of Mianchi County and Xinan County, 80° northeast, 16 km from Mianchi County, about 18 km from Xinan County, and 8 km from Yima City. The mining area is located in a low hilly land; the overall terrain is high in the west and low in the east. The center of the mining area is low in both high sides, with a regional height above sea level of 373.1–767.6 m and a maximum relative height difference of 384.5 m. The terrain slope is 15°–45°, and the general slope is about 25°^[16]. The mining area is located in the southern area of the Sino-Korean paraplatform in China and the Huaxiongtai promontory depression in Mianchi. The northwest area of the Queshan depression is folded off, the north wing strata of Mianchi is of monoclinic output, with a 170°–220° inclination, at an angle of 20°–40°, a general angle of 25°–32°, and the section changes slightly along the

strike. The strata belong to the North China stratigraphic region. In addition to the deletion of the Ordovician, Silurian, Carboniferous, and Permian strata, the strata since the Cambrian to Cenozoic era is exposed, with developing depositional sequence and a large thickness.

In the scope of Duan Village-Leigou monohydrallite goaf, private mining mines have characteristics such as mining in large quantities with a wide distribution, unclear mining history, *etc.* Therefore, the spatial distribution of the goaf and its state is very complex, with a serious threat to the smooth mine construction and safe mining^[17].

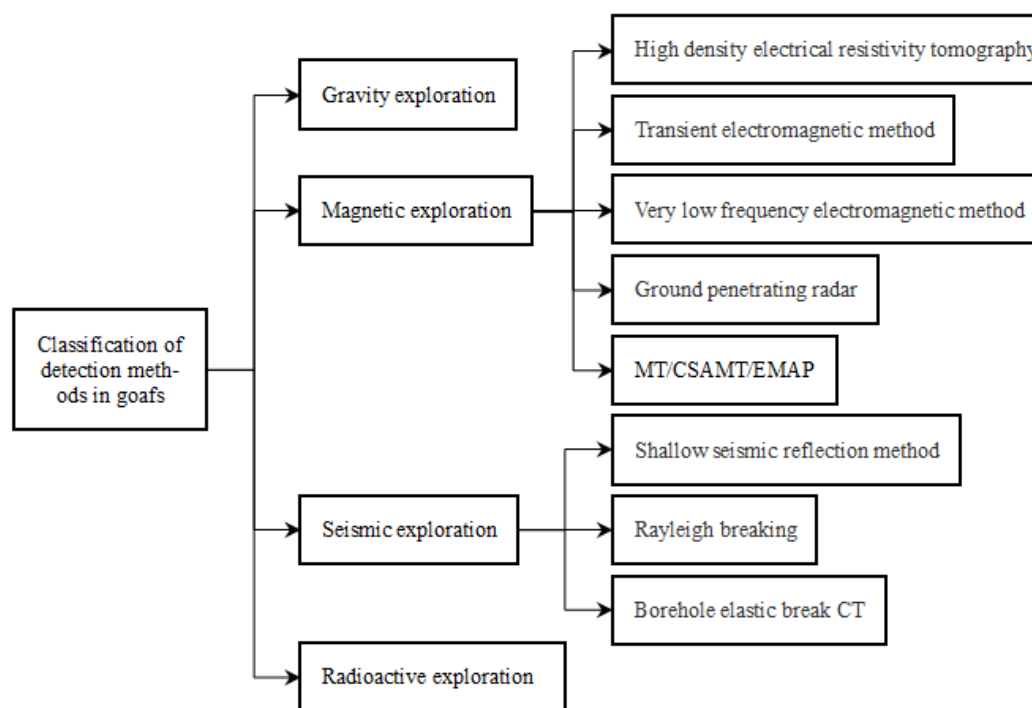


Figure 1. Classification of detection methods

Detection method theory and technological research in the study area

An effective geophysical exploration method is selected according to geological generalization and geophysical characteristics of the mining area, the size, and shape of the tunnel. Geophysical prospecting methods of the test mainly include seismic reflection, direct current method, high density^[18-21], earth electromagnetic imaging^[22], and radon emanation measurement.

Selection of test mines

After a survey of 88 mines in the Duan Village-Leigou monohydrallite area, the mines were chosen with relatively reliable materials of which the surrounding environmental conditions are known and geological generalization comply with the following several conditions chosen as test mines: 1) the site is broad and flat; 2) less electromagnetic interference; 3) simple geological structures; 4) depth of buried tunnel is moderate. A total of eight mines—54, 66, 118, 180, 183, 193, 199, and 266—were determined as test mines. The surrounding environment, geological model, and tunnel conditions are shown in *Table 1*.

Test method and results analysis

Different testing methods are selected to assess the test mines in this study. More comprehensive geological information was obtained via the information provided by the various geophysical places. Geological inference was made to con-

form to the objective conditions combined with geological data, drilling data, and so on. The scope and accuracy of different test methods are verified.

1) Seismic reflection

The test adopts the longitudinal measuring line 3 times to cover the observation system, move shot point, and acceptance point at the same time. The shoot off end, received 12 ways, 12 m in offset, at a detection distance of 2 m, moved two detection every time. The explosive was chosen as the source, dosage at 30–50 g, and the focal hole depth was 0.3–0.5m.

A measuring line 66dz1 was arranged around mine 66 in the experiment with a length of 100 m; a measuring line 193dz1 was arranged around mine 193 with a length of 122 m; 3 measuring lines 199dz1, 199dz2, and 199dz3 were arranged around mine 199 with a respective length of 146 m, 146 m, and 136 m. A measuring line 266dz1 was arranged around mine 266 with a length of 100 m. A round-trip time cross-section diagram of the seismic reflection was formed by managing 750 m reflection record of 6 measuring lines. The round-trip time cross-section diagram of seismic reflection for 199dz2 measuring line around mine 199 demonstrated that there is a synthetic shaft at 62.8 m, which is a bauxite layer by comprehensive analysis and inference. However, the connection of synthetic shaft at 52 m between the front and back is very good, with no anomalies of the synthetic shaft, such as distortion, deletion, incoherence and so on, which indicated no reflection on the round-trip time cross-section diagram of the tunnel. No corresponding anomaly was found for the cross-section diagram of the other 5 lines.

Table 1. Surrounding environment and tunnel condition of test mine

Mine number	Terrain	Buried tunnel depth (m)	Trend, length, number of roadway	Electromagnetic environment	Stratum characteristics
54	Highs and lows	54	Slightly north, under 28 m west, south-west, less than 35 m (downdip). 2 lines	No high pressure	Loess, lishi, pebble bed, shale, limestone, coal seam
66	Gentle hike	About 6	The northeast, 110 m. 1 line	No high pressure	Loess, clay rock
118	Flat lope	95	The northeast, 10 m; south, 70–80 m. 2 lines.	No high pressure	Loess, sandstone, shale, limestone, bauxite layer
180	Adjacent to the high earth station	44	West, 20 m, 9 m to the north, 12 m to the south, 6 m; 18 m to the north, 8 m. 1 line 3 lines	No high pressure	Loess, sandstone, shale, alumina layer
183	Subsidence	33	South, 10 m, leads to subsidence center	No high pressure	Loess, shale, 12 m ore
193	Flat	7	South, 30 to 40 m; west, 10–20 m; north 10–20 m. 3 lines.	No high pressure	Loess, shale, alumina layer
199	Small flat slope	22	Northwest, 6 to 7 m, and then to the south, 15 to 16 m. 1 line.	Near the domestic load	Loess, pebble bed, shale, alumina layer
266	Flat	45	The east, 50 m, west, 40 m. 2 lines.	No high pressure	Loess, pebble bed, shale, mudstone, alumina layer

2) Direct current method

In this experiment, the symmetrical quadrupole device was used to carry out the direct current test, and the work arrangement is shown in *Figure 2*.

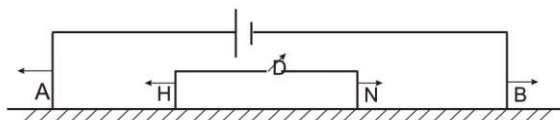


Figure 2. Symmetrical quadrupole probing device

The minimum power supply pole at pitch $AB/2$ is 4.5 m; the largest power supply pole at pitch $AB/2$ is 150 m; the minimum measuring pole at pitch $MN/2$ is 1 m; and the maximum measured pole at pitch $MN/2$ is 5 m. The corresponding relationship between $AB/2$ and $MN/2$ is shown in *Table 2*. With an iron electrode as the power supply electrode, a copper electrode as the measuring electrode, the multiple electrode power supply in parallel; filling and watering are adopted, or the grounding resistance is reduced by paralleling electrodes, locally with individual conditions connecting to the ground being poor. The grounding connection also improved. The maximum supply voltage reaches to 225 V using B cell as the power supply. The distance between sounding points is 10.0 m.

Table 2. Corresponding relation between power supply polar distance and test polar distance

$AB/2$ (m)	4.5	6	10	15	25	15	25	45	60	100	150
$MN/2$ (m)	1	1	1	1	1	5	5	5	5	5	5

A measuring line 66DF1 was arranged near mine 66 in the experiment with a length of 100 m and a measuring line 183DF1 was arranged near mine 183 with a length of 160 m. Four measuring lines 266DF1, 266DF2, 266DF3, and 266DF4 were arranged near mine 266 at a length of 100 m. The sounding apparent resistivity contour map was formed by processing electrical sounding data via direct current method of 660 m for 6 measuring lines. Results are shown in *Figure 3*.

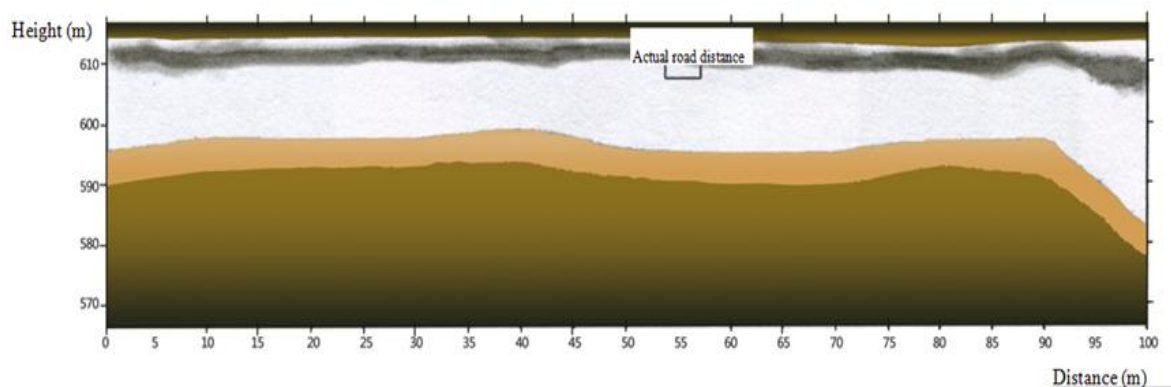


Figure 3. Typical sounding apparent resistivity contour map of direct current method

Figure 4 illustrates the sounding apparent resistivity contour map by direct current method for measuring line 66DF1 near mine 66. The geological layer of *Figure 4* is clear and consistent with the known data. There were no problems in detecting bauxite distribution and spatial characteristics via direct current method. According to the survey, there is a tunnel with a through depth of about 6.5 m (identified in *Figure 3* rectangular line) at 55 m of the 66DF1 measured line, but we deduced that there was no high or low abnormal resistivity in the bauxite layer from the graph. It showed that the effect of direct current sounding method to detect the tunnel is not sufficient. This was also observed in the other 5 lines.

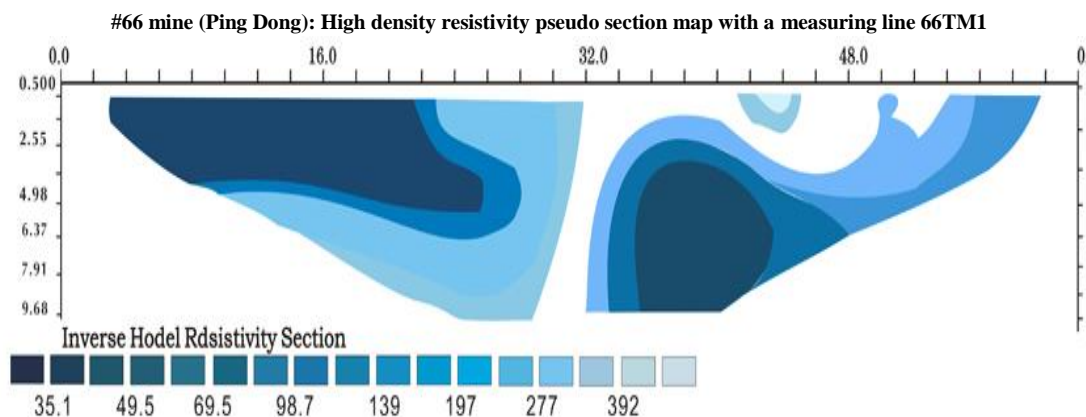


Figure 4. Typical resistivity pseudo section map of high density resistivity method

3) High density resistivity method

Due to the complexity of the device coefficient and parameter set for high density resistivity method, the test adopted 6 measuring lines, a Wenner device, and a 2 m electrode pole pitch. A measuring line 66TM1 was arranged around mine 66 in the experiment with a length of 62 m; 2 measuring lines 180TM1, and 180TM2 are arranged around mine 180, both with a length of 200 m; 2 measuring lines 183TM1, and 183TM2 were arranged around mine 183, both with a length of 194 m; a measuring line 199TM1 was arranged around mine 199 in the experiment, with a length of 158 m. The high density resistivity pseudosection map was formed by processing electrical sounding data via high density resistivity method of 1008 m for 6 measuring lines. The results are shown in *Figure 4*.

There is a high resistance body at a depth of 3.5m in the pile number at 34–40.0 m in *Figure 4*, which is consistent with the adit position in the scene and buried deep of the field survey.

The lithological distribution of mine 199 were: an upper formation of quaternary loess and pebble; a middle-upper gob fillings, with loess and clay rock as its main ingredients; a central bauxite layer, with pewter, oolitic and block structures; an empty area at 18.44–22.13 m; gob fillings (solid filling) at 22.13–23.23 m; and ferruginous clay rock at 23.33–37.25 m. In *Figure 5*, the pseudosection map stratified clearly the bauxite horizon and is easily distinguished by integrating the known data. There is a high resistance body at a depth of 22.0 m in the pile number at 95.0 m, which is consistent with the position of the tunnel in the field survey.

Resistivity of the quaternary overburden layer is low and is generally loose when filled with water. Underground goaves can be divided into three categories in general, depending on its fillings: (1) air filling, with a theoretical high resistance resistivity; (2) groundwater filling, with a theoretical low resistance resistivity; (3) mixed filling, filling medium include gravel, soil, air, water, *etc.* Theoretical resistivity levels are between the two filling types mentioned^[12]. Identifying resistivity levels is a geophysical prerequisite of using high density resistivity methods to probe goaves.

No abnormality was found in resistivity pseudosection maps for the 4 measuring lines 180TM1, 180TM2, 183TM1, and 183TM2. However, according to the survey, there was a tunnel through all the measuring lines. In our analysis, the tunnel may be buried too deep, limiting the power supply voltage of our current instrument, causing low abnormal signal-to-noise ratio in the tunnel.

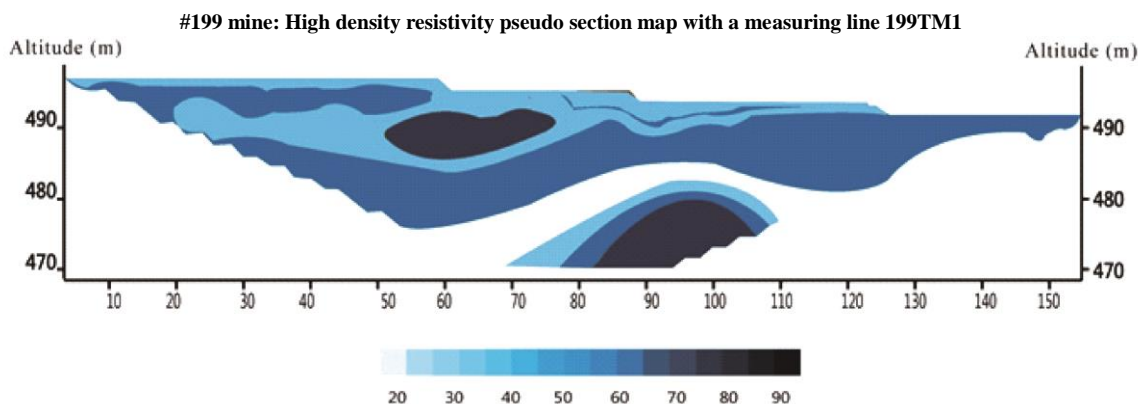


Figure 5. Typical resistivity pseudosection map of high density resistivity method

From the inversion processing result based on the high density resistivity method in the experimental area, the electrical characteristic of the study area is characterized with low resistance. Low resistance and low speed are the main features in the identification of goaves.

4) Earth electromagnetic imaging (EH-4)

Four census survey lines were arranged in order to explore the working method and familiarize with the electrical characteristics of the mining area formation, with polar distance and dot pitch of 10 m along line numbers EH-4-SY1, EH-4-SY2, EH-4-SY3, and EH-4-SY4, at a respective length of 840 m, 940 m, 720 m, and 750 m. The experiment proceeds by reducing polar distance and dot pitch gradually, with consideration on work efficiency and resolution detection.

Initially, at a polar distance of 10 m and dot pitch of 5 m, 3 measuring lines were arranged near mine 266, with line numbers 266EH1, 266EH2, and 266EH3, all at a length of 90 m each. Then, 3 measuring lines with a polar distance of 10 m and dot pitch of 3 m were arranged, with line numbers 266-EH1, 266-EH2, and 266-EH3, at a length of 90 m each. Three measuring lines were also arranged near mine 118 with a polar distance of 5 m and a dot pitch of 3 m, with line numbers 118EH1, 118EH2, and 118EH3, at a length of 108 m each. Then, 3 measuring lines were arranged near mine 118 with a polar distance of 3 m and a dot pitch of 3 m, with line numbers 118-EH1, 118-EH2, and 118-EH3, at a length of 108 m each. Finally, a measuring line 54xb1 was arranged near mine 54, with a length of 20 m.

The EH-4 resistivity pseudosection map was formed by processing earth electromagnetic imaging data (EH-4) of 4458 m for 17 measuring lines. Results are shown in *Figures 6*.

Figure 6a shows the resistivity pseudosection of EH-4-SY1 measuring line (part). According to the field survey, we found a tunnel at 95 m, buried deep at a depth of 44 m of the line; however, there is no abnormality in the figure.

In *Figure 6b*, there was abnormally high resistance below the depth of 60 m in the pile number at about 40.0 m, which is consistent with the adit position in the scene and after depth correction, is buried deep in the field survey. However, the tunnel is abnormally fuzzy and is not easily identified.

Figure 6c is a pseudosection map and after further reducing the polar distance and dot pitch, the clear stratification can be seen. The bauxite layer is easily identified and the tunnel anomaly is obvious. The figure shows that there is a low resistivity anomaly in the buried depth of 54.0 m and about 10 m on the line, which was proven to be caused by groundwater-filled tunnels through drilling. It is consistent with the tunnel on survey.

Overall, in the pseudo section map for 10.0 m dot pitch with no tunnel reflection; detection effect for 3.0 m and 5.0 m dot pitch is not ideal and the abnormality is fuzzy; an effect at 2.0 m dot pitch is the best.

5) Radon emanation survey

The test dot pitch was at 5.0 m. A measuring line of 66fsx1 was arranged around mine 66 with a length of 100 m; 3 measuring lines, 266fsx1, 266fsx2, and 266fsx3 were arranged around mine 266, at a length of 80 m each.

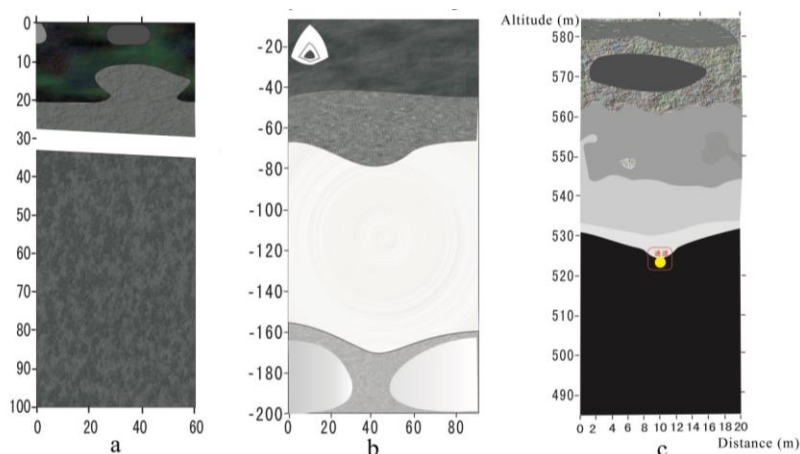


Figure 6. (a) The EH-4 resistivity pseudo section map with SY1 measuring line; (b) Resistivity pseudo section map with 266EH1 measuring line; (c) Resistivity pseudo section map with 54XB1 measuring line

The resulting map of the pulse counting-distance curve is drawn by processing radon emanation survey data of 340 m for 4 measuring lines. Results shown in *Figure 7* is the map of the radon emanation survey for measuring line 266fsx2 around mine 266. According to the survey, there is a tunnel at a buried depth of 45.0 m and 68 m on the line (*Figure 7*). However, *Figure 7* shows that the pulse count of the whole measuring line is stable and less volatile, with a maximum value of 27, a minimum value of 21, and an average value of 25. There is no pulse counting mutation caused by the tunnel at 68 m of measuring line. The other three lines are similar; it shows that the effect of radon emanation survey is not good.

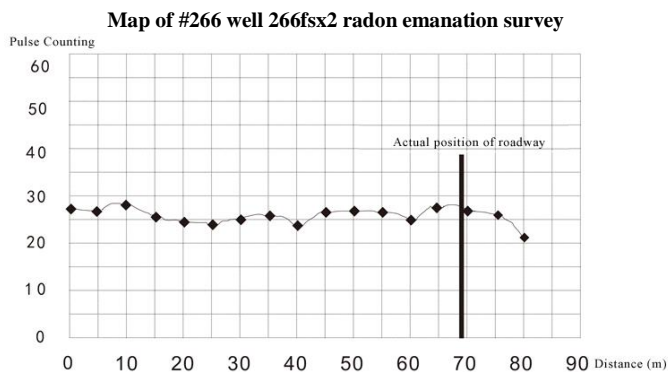


Figure 7. Results of the radon emanation survey

Effect analysis of test results

In this study, we selected 8 mines of known cases, laid 39 lines and used 5 geophysical prospecting methods. The test results are as follows:

- 1) Seismic reflection (total 6 survey lines, 750 m); direct current method sounding (a total of 6 survey lines, 72 dots). The two methods gave clear stratification and detected the bauxite layer in the area. However, this technique is not ideal for finding tunnel positions and filling conditions of tunnels.
- 2) High density resistivity method, a total layout of 6 measuring lines with a total length of 1018.0 m. Test results showed that application effect for shallow goaf was better in the area, especially the detection effect on a tunnel

buried deep within 20.0 m. From high and low resistance reflections in the resistivity quasi section maps, the space position and filling condition of the tunnel can be accurately judged, the geological stratification is clear, and the bauxite layer reflection is obvious. However, for the target body of a buried depth above 20.0 m, its detection effect is not good.

- 3) Earth electromagnetic imaging (EH-4). The experimental workload is larger; a total of 17 measuring lines were tested; the cumulative length of the measuring line was 4488.0 m. The adopted dot pitches were: 10.0 m, 5.0 m, 3.0 m, and 2.0 m. Experimental results showed that geological stratification effects of the 4 kinds of dot pitch probes were good, with clear reflection of the bauxite layer. Nevertheless, detection effect for 10.0 dot pitch was not sufficient, tunnel space position could not be reflected out; detection effects for 3.0 m and 5.0 m dot pitches were also not ideal, goaf is abnormally fuzzy. The detecting effect of tunnel buried deep above 20.0 m with the 2.0 m dot pitch was very good and the anomaly reflection was clear. Detecting resolution improved as polar distance and dot pitch reduces. It should be pointed out that, the diminution of the polar distance and dot pitch can reduce the overall effect of a geological body under the measuring point and highlights the target signals, but it is not unlimited. Because the target body signals are also reduced as the polar distance and dot pitch reduces, especially for large buried depth target bodies, the target signal may be too small to be distinguished by the instrument when the polar distance and dot pitch is reduced to a certain degree. The space position of the tunnel can be accurately judged from the anomaly reflection on the resistivity section map. The filling condition can be judged according to the abnormal high and low resistances.
- 4) The radon emanation survey (four lines of 340 m) was originally used to locate goaf boundaries (should be relatively ideal), and later due to the change in the detection purposes, it was used to locate tunnels, but the effect was not ideal and test results have proven this.

Conclusion

After a comprehensive analysis of five kinds of detection methods, we conclude that: the tunnel should adopt a high density detection method with a polar distance of 2.0 m, at a depth of around 20.0 m or less than 20.0 m. For tunnels with a buried depth above 20.0 m, the earth electromagnetic imaging method (EH-4) is appropriate with a dot pitch and polar distance of 2.0 m. Mines 189 and 187 should be measured using the high density method, but the earth electromagnetic imaging (EH-4) method was used, thus limiting the working area, but this has also achieved a good effect.

Summary and outlook

On the basis of principles, characteristics, and applicability of various geophysical methods in the system analysis, and in view of the characteristics of different goaf depth and the requirements for the high resolution detection, this study adopts the combination of five kinds of methods, through a variety of geophysical exploration methods to authenticate each other, which make up for the limitations of a single method^[23].

There are places worth studying to detect goaves. For situations of abnormal high resistance of goaf filling, only the use of geophysical exploration method for determining fillings is quite difficult in terms of the current domestic level, and it is recommended to cope with drilling sampling. As the measuring line density in the practical engineering can't be too small, there may be some errors in the test of tunnel length. The error can be further reduced if the length of the measuring line increases. At present, goaf detection technology has made some achievements. However, due to the particularity of the goaf, limitations, and multiple solutions of geophysical methods, the traditional single detection method and the single content cannot meet the needs of the project. We need to establish mathematical physics model of all methods and optimize detection methods according to the characteristics of the goaf, which is still an issue to be further studied^[24,25].

References

1. Li XB, Li DY, Zhao GY, Zhou ZL, Gong FQ. Detecting, disposal and safety evaluation of the underground goaf in metal mines. *J Mining Saf Eng* 2006; 23(1): 24–29.
2. Kong XY, Liu J, Huang B, Sun R. Analysis and research on prediction of foundation deformation of Wangr shan mined-out area of Jiaojia gold mine. *Gold* 2012; 33(3): 27–31.
3. Guo GL, He GQ, Cui SQ. The stability analysis for the covered rock mass in some abandoned mine-out areas. *Ground Press Strata Control* 2003; 20(3): 70–73.
4. Sun ZD. Evaluation and treatment of the exploration and damage degree of the hole under the high grade highway. Beijing: Science Press; 2000.
5. Information research room of geochemical exploration institute of geophysical ministry. Japanese engineering geophysical technology anthology in translation. Beijing: Information Research Room of Geochemical Exploration Institute of Geophysical Ministry; 1984.
6. Wang L. Application of shallow seismic reflection wave method in the exploration of high dip coal seam. *Xinjiang Geol* 1998; 16(3): 280–282.
7. Liu DW, Gu DS, Xu GY. Evaluation and optimization of disposal methods for gob in underground mine. *China Mining Mag* 2004; 13(8): 52–55.
8. Wang ZD. Application technology of shallow seismic exploration. Beijing: Geological press; 1988.
9. Liu J. Application of transient electromagnetic method in detecting coal mine goaf. *Sci Technol Inform Dev Econ* 2005; 15(16): 281–282.
10. Yu GM, Li J, Han GM. Application of comprehensive geophysics in detection of mined-out area in deep coal- seam. *Geol Shaanxi* 2003; 21(2): 62–69.
11. Chen LS, Wang GE. Method of ground magnetic survey. Beijing: Geological press; 1990.
12. Ding RS, Zhang DC, Wang SC, Ma HH, Zheng Q, *et al.* The application of high-density resistivity method and seismic image method to the exploration of exhausted areas. *Geophys Geochem Explor* 2010; 34(6): 732–736.
13. Jin JS. The methods of seismic exploration delineation of gob area. *Coal Geol China* 1998; 10(3): 7.
14. Guo CG, Li JY, Liu J. The application of radon measurement mining empty area in Shanxi. *Sci Technol Inform Dev Econ* 2004; 14(1): 180–181.
15. Yang FJ, Liu QD. Application of comprehensive parameters of electric method in geothermal prospecting within Silapu region, Liaoning. *Miner Resour Geol* 2004; 2004(04): 383–387.
16. Wu LF. Duan village-Leigou exploration of bauxite mining plan. *Mining Technol* 2010; 11: 6–7, 29.
17. Li YJ, Huang BY. Analysis of geological characteristics and genesis of bauxite at DuanCun-Leigou, Henan. *Conserv Util Miner Resour* 2013; 26(2): 10–14.
18. Lu YX, Wang Y, Xu YX, Zhou ZQ, Zhai FZ. Application in surveying of underground caves by high-density resistivity method. *Chin J Eng Geophys* 2010; 7(6): 674–678.
19. Meng GX, Yan JY, Lv QT, Zhang K, Chen WM. The application of electrical resistivity imaging in stone mineral deposits exploration. *J Jilin Univ (Earth Sci Ed)* 2010; 41(2): 592–599.
20. Song XL, Gong SL, Xin LT, *et al.* Applications of high- density electrical method to underground cavity detection. *Chin J Eng Geophys* 2010; 7(5): 599–602.
21. Zhang XY, Bi BK, Yang PT, Wu YL, Shen SS. The application of the high density resistivity method to the survey of the mined-out area. *Geophys Geochem Explor* 2009; 33(3): 309–312, 326.
22. Tan HD, Yu QF, Booker J, Wei WB. Three dimensional rapid relaxation inversion for the magnetotelluric method. *Chin J Geophys* 2003; 46(6): 850–854.
23. Wang HF, Liu RQ, Zheng Q, Chen YG, Guo D, *et al.* Application of comprehensive geophysical prospecting in the metal mine goaf—in Jiaojia gold Wangershan goaf as an example. *Geol Explor* 2013; 49(3): 496– 504.
24. Duan ZY. Exploration investigation and practice of abandoned well treatment. *J Kunming Metall Coll* 2001; 17(2): 3–4.
25. Zhu BJ, Hao ZD, Zhang YL, Ou YM. Inspecting and dealing in goaf. *Opencast Coal Mining Technol* 2002; 3: 39–40.